Density Functional Theory Study of Triphenyl Phosphite: Molecular Flexibility and Weak Intermolecular Hydrogen Bonding

Olivier J. Hernandez*,† and Abdou Boucekkine‡

Equipe Matériaux Inorganiques: Chimie Douce et Réactivité, et Equipe Chimie Théorique Inorganique, Sciences Chimiques de Rennes, UMR 6226 CNRS−Université de Rennes 1, Bât. 10B, campus de Beaulieu, 263, avenue du Général Leclerc, F-35042 Rennes, France

Alain Hédoux

Laboratoire de Dynamique et Structures des Matériaux Moléculaires, UFR de Physique, UMR 8024 CNRS−Université de Lille 1, Bât. P5, F-59655 Villeneuve d'Ascq, France

Received: March 9, 2007; In Final Form: May 21, 2007

The high conformational flexibility of triphenyl phosphite (TPP) is investigated by density functional theory (DFT) calculations. First, through a scan of the molecular potential energy surface, we bring to light a new stable conformation of an isolated molecule, not yet encountered in the crystal states of TPP. Different relevant conformations of the TPP monomer in the gas state are further presented and discussed in terms of molecular structure, relative energy, and dipole moments. Second, we considered dimer and trimer of TPP starting from their structural topology within the hexagonal crystal, which is characterized by the existence of molecular rods. It is shown that weak C−H···O intermolecular hydrogen bonds in TPP cannot definitely be excluded, and finally this point is discussed in the scope of the glacial state problem.

1. Introduction

Triphenyl phosphite [TPP, $P(OPh)_3$] is a simple molecular liquid at room temperature that is more and more used as a ligand in organometallic chemistry due to its stronger π-electroacceptor properties and to its smaller steric hindrance than triphenyl phosphine (PPh_3),[1] phenyl rings being indeed very flexible along the C−O−P bond.[2] Among the published TPP organometallic complexes, quite different conformations of the $P(OPh)_3$ moieties are indeed encountered in the solid state, illustrating the high conformational flexibility (six degrees of torsional freedom) of this molecule.

On the other hand, from a phase transition point of view, this fragile glass-forming molecular liquid has been intensively studied since the discovery by Kivelson and co-workers,[3,4] at ambient pressure and in a very accessible temperature range between the melting point (T_m = 297.7 K) and the glass transition (T_g = 201.8 K),[5] of a new apparently amorphous solid phase, named glacial state (GS), different from the normal liquid, supercooled liquid, and glassy states. TPP was then considered as a prototype system for studying polyamorphic transitions (i.e., first-order transitions between two different amorphous states), since it can be analyzed by usual laboratory equipment, whereas for other examples (e.g., H_2O, liquid phosphorus) the polyamorphic transition is observed under extreme conditions (high pressure and low or high temperature). The GS, metastable with respect to the crystal state, appears typically between 210 and 230 K from the supercooled liquid through a first-order phase transition (i) by slow heating (less than 1 K·min^{-1}) from the glassy state; (ii) by rapid heating (ca. 10 K·min^{-1}) again starting from below T_g (or by direct quench from above T_m) to an aging temperature (T_a) where the GS is isothermally formed on the time scale of several minutes to hours depending on T_a. Numerous experimental studies have tried since 1996 to get a better insight into the nature, the real local structure, the homogeneity, and the origin of this intriguing GS. The main descriptions of the GS at present are summarized hereafter.

According to Kivelson and Tarjus and co-workers,[6−8] the GS would be a poorly crystallized defect-ordered phase constituted by polydisperse nanocrystallites (typically 100−250 Å) of a plastic crystal (thus with a local arrangement of the molecules different from that of the crystal) with a large unit cell (80 Å) embedded in an interstitial liquid, in agreement with the frustration-limited domains (FLD) thermodynamical theory of supercooled liquids.[9] Another heterogeneous description for the GS is proposed by Hédoux et al., whereby the GS would be a biphased phase constituted by a mixture of nano- to microcrystallites—depending on T_a, amorphous-like GS for 210 < T_a < 216 K and crystal-like GS for 216 < T_a < 230 K—of the hexagonal crystal phase embedded within untransformed supercooled liquid, forming a heavily nucleated state.[10,11] Tanaka et al.[12,13] considered also two regimes within the temperature range where the GS is formed. Below a spinodal-decomposition temperature (T_{SD} ~ 216 K), a homogeneous phase is observed: the GS would be the glassy state of a second liquid II (glass II). Above T_{SD}, the observed phase is heterogeneous, and the GS would be a mixture of glass II and microcrystallites of the crystal phase. The existence of a liquid−liquid phase transition is speculated, in this instance between liquid I and glass II. Senker, Rössler, and co-workers[14−17] argued that for T_a > 223 K a nano- or microcrystalline material is formed, whereas for T_a < 223 K the GS is homogeneous and disordered. According to these authors, the GS is described as a second highly viscous liquid-phase exhibiting structural correlations in terms of small

* Corresponding author: e-mail olivier.hernandez@univ-rennes1.fr.
† Equipe Matériaux Inorganiques: Chimie Douce et Réactivité.
‡ Equipe Chimie Théorique Inorganique.

10.1021/jp071934d CCC: $37.00
Published on Web 06/29/2007

clusters of preferentially parallel aligned molecules. For the sake of completeness, two other but discontinued studies on the GS should be cited. For Johari and Ferrari,[18] the GS appears to be similar to a plastic crystal or to a liquid crystal but they also stated that the crystal phase is a plastic crystal, which is obviously not relevant; the hexagonal crystal phase is nowadays accurately characterized[19,20] and displays no significant disorder. On the other hand, Oguni and co-workers[21] concluded, as did Senker, Rössler, and co-workers, that the GS is a highly correlated second liquid.

Whether the GS is a true homogeneous amorphous phase or not is still a matter of debate; we hope to determine whether TPP could be really a candidate for true polyamorphism and for the first observation of an amorphous−amorphous phase transition under ambient conditions.

According to powder X-ray synchrotron diffraction and Raman spectroscopy experiments, the possibility of weak intermolecular C−H···O hydrogen bonds in the hexagonal crystal phase at 110 K[20] as well as in the GS at 222 K[22,23] (even though with subtly different characteristics of these hydrogen bonds between the two phases) has been first suggested by Hédoux and co-workers.[22,23] This kind of additional stabilizing force in TPP is ruled out by certain authors[14,15,19] but was recently corroborated by Benmore and co-workers,[24] who studied the local structure of the different condensed phases of TPP by means of high-energy X-ray and spallation neutron scattering experiments. They have shown by the hydrogen/deuterium first-order difference method that the crystalline spectra display, with regard to the glass and supercooled liquid ones, additional hydrogen correlations at ∼3 and 3.4 Å, mostly due to inter-phenyl ring H−C/H interactions. Those interactions could be associated in part with weak intermolecular hydrogen bonds that turned out to be present in the crystal phase but not in the glass nor in the supercooled liquid as previously shown by Hédoux and co-workers.[22,23] It is also reported that the molecular conformations (probably the C−O/P interactions) in the crystal and in the GS, as well as the P···P contact distances, are different. Finally Benmore and co-workers stated that the GS spectra cannot be described as a simple mixture of supercooled liquid and crystalline components (interpretation of Hédoux and co-workers). They conclude that competition between optimum molecular conformation and weak intermolecular hydrogen bonds would be responsible for the existence of the GS in terms of abortive crystallization attempt. The same group further interpreted new combined high-energy X-ray and spallation neutron diffraction data by means of the reverse Monte Carlo modeling technique.[25] It is shown that the GS can be structurally modeled as a disordered phase very close to the supercooled liquid and characterized by three typical modes of orientational correlations between nearby phenyl rings of different molecules. But the GS is able to form unusually weak intermolecular C−H···O hydrogen bonds (contact distances of ∼2.75 Å) between antiparallel phenyl rings that are not present in the supercooled liquid and that are topologically different from those encountered in the hexagonal crystal state.[20]

In order to explore the most stable molecular conformations and to clarify the type of supermolecular correlations (van der Waals, C−H···π, hydrogen bonds?) we are dealing with in the different phases of TPP, we have performed a quantum chemistry theoretical study of TPP in the gas state (i.e., without taking account any periodicity) at 0 K through the density functional theory (DFT, Gaussian03 code).

First, different relevant conformations of the TPP monomer in the gas state are presented and discussed in terms of molecular structure, relative energy, and dipole moments. A partial molecular potential energy surface is proposed by scanning two relevant dihedral angles and optimizing step by step the molecular conformation, revealing the occurrence of a new stable conformation not yet encountered in the crystal states of TPP. In a second stage, we have built dimers and trimers of TPP starting from the structural topology within the hexagonal crystal,[20,19] that is, the existence of antiparallel molecular rods directed along the shortest *c*-axis, and forming a hexagonal array. It is shown that weak C−H···O intermolecular hydrogen bonding in TPP can definitely not be excluded, and finally this point is discussed in the scope of the GS problem.

2. Computational Details

It is well-established that DFT techniques using, for instance, B3LYP[26] or MPW1PW91[27] exchange-correlation functionals and suitable basis sets can lead to an accurate prediction of bond lengths and angles and molecular conformations via geometry optimizations. The latter functional, which is a modified Perdew−Wang one, is well suited for nonbonded interactions and transition-state studies and leads to results that are as reliable as B3LYP's concerning ground-state properties.[27] For our part, unless otherwise specified, we made use of the MPW1PW91 functional with the standard polarized triple-ζ 6-311G**. We expect that this level of computation should be accurate enough in our case, especially because of the suspected occurrence of intermolecular hydrogen bonding in the hexagonal crystal state.[20] When intermolecular interaction energies between two or three TPP species were computed, the basis set superposition error (BSSE) was taken into account by use of the counterpoise recipe. All calculations have been performed with the Gaussian03 software package.[28]

3. Results and Discussion

3.1. TPP in the Gas Phase. The molecular geometry of TPP in the hexagonal crystal state[20,19] displays roughly a C_s symmetry (see Figure 4 of ref 20). We started our study by building from the experimental conformation an idealized TPP molecule with a strict C_s symmetry (Figure 1). Intuitively, a C_3 conformation (Figure 2) can also be considered for an isolated TPP molecule if a symmetric propeller shape is taken into account. We carried out geometry optimizations on both conformations. We found that both geometries are thermodynamically stable, as they exhibit real vibration frequencies, although the C_s conformation appears significantly more stable than the C_3 one (difference in energy of 4.7 kcal/mol). Moreover, the two geometries display very different features in terms of dipole moment: the C_s form is almost not polar ($\mu = 0.17$ D) while the C_3 form is strongly polar, $\mu = 1.61$ D, with the dipole moment directed along a direction perpendicular to the plane formed by the three oxygen atoms and passing through the P atom (actually directed along the direction defined by the phosphorus atom and its lone pair; Figure 2b).

As stressed in the Introduction, due to the presence of six torsion angles (see Figure 1 of ref 20), likely with low barriers of rotation, the TPP molecule displays huge conformational flexibility, leading to different possible conformations. For that reason we carried out, by means of standard B3LYP/6-31G* calculations—similar results being obtained with the MPW1PW91 functional—a partial two-dimensional scan of its molecular potential energy surface, starting from the C_s geometry and considering as variables the τ_1 and τ_2 dihedral angles (Figure 1a). Up to 99 conformational optimizations have been performed, with the initial values for τ_2 varying from 38° to −42°

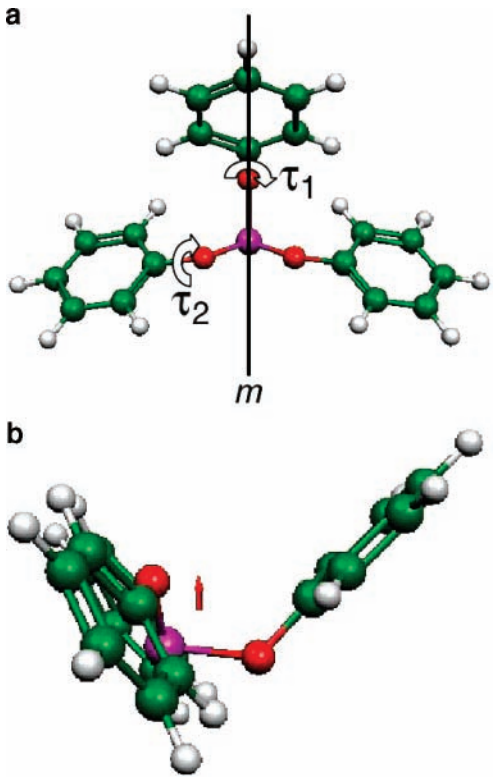

Figure 1. C_s TPP monomer from DFT calculations: (a) view along the dipole moment axis; (b) perpendicular view. In panel a, the two dihedral angles C−C−O−P τ_1 and τ_2, used for scanning the partial molecular potential energy, and the molecular mirror plane noted *m* are indicated. The dipole moment is drawn.

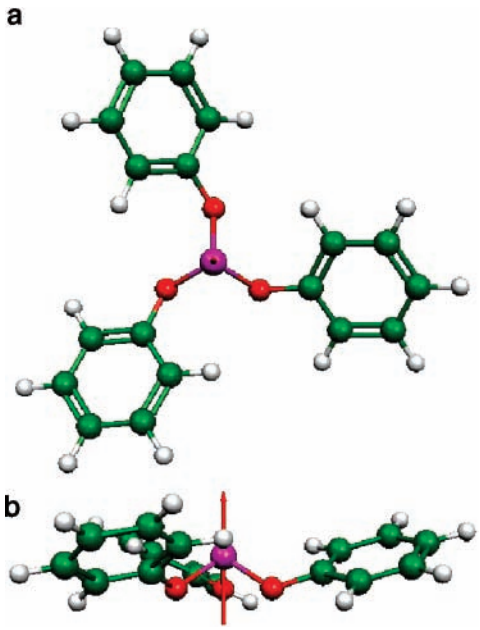

Figure 2. C_3 TPP monomer from DFT calculations: (a) view along the dipole moment axis; (b) perpendicular view. The dipole moment is drawn.

in steps of 10° and from 90° to −60° in steps of 15° for τ_1. The so-obtained molecular potential energy surface of TPP is shown in Figure 3. This study, which is not exhaustive due to the unreasonable calculation time required for exploring all the conformational space, reveals a more stable structure than the previous C_3 and C_s ones, exhibiting C_1 symmetry (Figure 4). The three geometries of the TPP molecule are located on the potential energy map of Figure 3. An energy barrier roughly

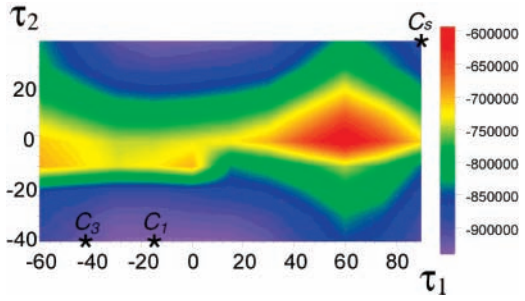

Figure 3. Partial molecular potential energy map from B3LYP/6-31G* calculations. The energy is given in arbitrary units. The three typical conformations of TPP (C_s, C_3, C_1) are located on the map. The energy in atomic units (au; 1 au = 627.51 kcal/mol) is equal to −1262 + (energy in arbitrary units) × 10^{-8}.

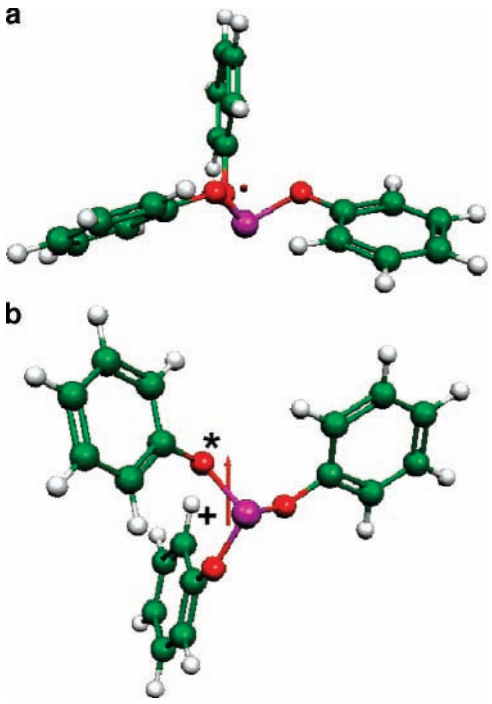

Figure 4. Most stable C_1 TPP monomer from DFT calculations: (a) view along the dipole moment axis; (b) perpendicular view. The dipole moment is drawn.

independent of τ_1 and corresponding to values of τ_2 around 0° is clearly observed. This barrier corresponds to a conformation with a lateral phenyl ring (with respect to the mirror plane) in the same plane as the corresponding P−O−C plane. A path from the C_s to the C_3 conformation, at least within the scanned potential energy surface, passes through this energy barrier. Moreover, about $\tau_2 \sim -40° \pm 10°$ and $\tau_1 \sim 0° \pm 40°$ (area centered around the most stable C_1 structure), a large and rather elongated potential energy valley is revealed where several stable conformations could be observed, at least in the gas phase, without being necessarily geometrically close even though they appear as neighbors on the 2D potential energy map, simply due to the fact that the four other dihedral angles of the TPP molecule are able to change significantly in the course of the DFT optimizations.

In Table 1, we report the relative energies and dipole moments of the three conformations we computed for an isolated TPP molecule (C_s, C_3, and C_1). The most symmetric C_3 geometry is clearly the less probable conformation in the gas state. The three P−O distances are equal to 1.651 Å, and the PO_3 pseudotetrahedron is characterized by an O−P−O angle of 96.3°. P−O−

TABLE 1: Different Molecular Conformations of an Isolated TPP Molecule after MPW1PW91/6-311G DFT Optimization**

form/symmetry[a]	absolute energy[b] (au)	absolute energy (kcal/mol)	relative energy (kcal/mol)	dipole moment (D)
C_1	−1261.716 474	−791 096.2292	0.0	0.73
C_s	−1261.714 809	−791 095.1852	1.04	0.17
C_3	−1261.707 319	−791 090.4890	5.74	1.61

[a] The C_1 geometry corresponds to the most stable form found throughout the scan of the partial molecular potential energy surface (see text). [b] One atomic unit (au) = 627.51 kcal/mol. The energy corresponds to the sum of electronic and thermal energies.

TABLE 2: Different C_1 Molecular Conformations of the TPP Molecule after MPW1PW91/6-311G Geometry Optimizations[a]**

form	absolute energy[b] (au)	absolute energy (kcal/mol)	relative energy[c] (kcal/mol)	dipole moment[d] (D)
hexagonal C_1	−1261.714 808	−791 095.1846	1.04	0.17 (0.45)
monoclinic C_1	−1261.715 827	−791 095.8235	0.41	1.44 (1.57)

[a] Optimizations were performed starting from the hexagonal[20,19] and monoclinic[30] geometries found in both crystal polymorphs. [b] One atomic unit (au) = 627.51 kcal/mol. The energy corresponds to the sum of electronic and thermal energies. [c] With respect to the most stable form found for an isolated TPP molecule throughout the scan of the partial molecular potential energy surface (C_1 geometry of Table 1). [d] The dipole moment before DFT optimization (i.e., strictly speaking, the one in the crystal state) is indicated in parentheses.

C−C (τ-type dihedral angle), corresponding to the rotation of the phenyl group around an axis constituted by the O−C bond, is equal to 145.7°; and C−O−P−O (α-type dihedral angle), corresponding to the precession of the O−C bond around the P−O axis at fixed P−O−C angle (in this instance at 122.2°), is equal to 93.2°.

For the less symmetric C_s geometry, the P−O bond belonging to the mirror plane (*m* in the following; see Figure 1a) is slightly shorter than the two others related by *m* (1.647 versus 1.654 Å). Notice that the averaging of those values gives the P−O bond length of the C_3 structure. Correlatively, the O−P−O angle perpendicular to *m* (91.4°) is much shorter than the two others that are mirror-related (101.8°), and the P−O−C angle with the O atom belonging to *m* is greater than the two others (126.0° against 121.6°). Interestingly, it appears that one phenyl ring on one side of *m* is characterized by practically the same τ and α angles (147.6° and 91.9°, respectively) as those encountered for the C_3 geometry (see above). Obviously its mirror-related counterpart displays opposite values for the τ and α angles. Both latter groups point above the plane defined by the three oxygen atoms. It means that the conformational transformation from the C_s to the C_3 structure leaves one phenyl ring unchanged and implies the modification of four dihedral angles instead of six. For the phenyl group passing through *m*, $\tau = 91.5°$ and $\alpha = 47.0°$; namely, this ring is perpendicular to the mirror plane and points below the plane of oxygen atoms.

The C_1 geometry is slightly but substantially more stable than the C_s one (difference in energy of only 1.1 kcal/mol) and exhibits a much higher dipole moment (0.73 versus 0.17 D). This effect can be easily understood if one takes into account the fact that two phenyl rings of the C_1 structure can very closely be superimposed to those of the C_3 geometry (τ angles of 142.2° and 143.6°, α angles of 90.4° and 94.1°, to be compared to 145.7° and 93.2°, respectively, for the C_3 geometry). Hence the conformational difference between the C_1 and C_3 structure lies in the value of "only" two dihedral angles, belonging moreover to the same phenyl group. More specifically, this specific phenyl ring ($\tau = 162.0°$ and $\alpha = 56.6°$) points below the oxygen atoms plane and is roughly perpendicular to the O−P−O angle of the C_3-type phenyl groups. The H atom in ortho position of the former phenyl group (indicated by a plus in Figure 4b) displays a particular arrangement characterized by three short contact distances with the three O atoms (2.447, 2.663, and 2.707 Å) and a localization directly below the P atom. The shortest of the three latter H···O contact distances is much shorter than the sum of the mean van der Waals radii for O and H (1.52 and 1.20 Å, respectively[29]), that is, 2.72 Å; the associated C−H···O angle is equal to 121.8°. The C_1 structure seems therefore to be stabilized by an intramolecular C−H···O hydrogen bond. Notice that the P−O bond of this group (distance of 1.629 Å) is shorter than the two others (1.650 and 1.673 Å) and the associated P−O−C angle is higher than those of the two C_3-type phenyl groups (132.2° versus 121.2° and 122.4°). The dipole moment lies within the plane of oxygen atoms (therefore is perpendicular to the dipole moment of the C_3 monomer) and is parallel to the O···O direction, with one O atom of C_3 type (indicated by an asterisk in Figure 4b).

3.2. TPP in the Crystal State. The situation could be different in the solid state, because of environmental and packing effects. To date, two crystal structures of TPP have been isolated. The first polymorph (hexagonal symmetry) is well characterized in the works of Senker and Lüdecke[19] and Hernandez et al.[20] Recently, Golovanov et al.[30] have isolated a second polymorphic modification (in this instance of monoclinic symmetry), metastable with respect to the first one, through the rapid cooling at 140 K of a 1:1 mixture of a highly polar solvent (i.e., ionic liquid; 1-butyl-3-methylimidazolium bromide) with liquid TPP.

Our DFT geometry optimizations of both polymorphs are reported in Table 2. Concerning the hexagonal modification, the final structure (hexagonal C_1, Figure 5) is highly similar (in terms of conformation, energy, and dipole moment) to the C_s geometry even though the C_s symmetry was not beforehand required. It is worth pointing out that although the geometry of the hexagonal polymorph before optimization (i.e., in the hexagonal crystal state) appears close at first sight to the hexagonal C_1 structure, the two molecules display different dipole moments: 0.17 D for the latter versus 0.45 D for the former. The DFT optimization of the conformation observed in the hexagonal crystal state leads therefore to a strong decrease of the molecular dipole moment as well as to a change of its relative orientation. This significant difference between the structures arises mostly from different values of the τ dihedral angle for one lateral phenoxy group (15.5° against 34.1°) that slightly breaks the mirror symmetry. This slight difference of about 19° for one torsion angle between the DFT-optimized hexagonal C_1 geometry (gas state) and the geometry encountered in the hexagonal crystal explains the aforementioned variations in the molecular dipolar properties and may be directly attributed to the intermolecular interactions occurring in the solid. Small variations of the TPP conformation have thus a nonnegligible impact on the molecular dipole moment. We confirm the assertions of Senker and Lüdecke,[19] whereby the dipole moment of the TPP molecule in the hexagonal crystal is moderately

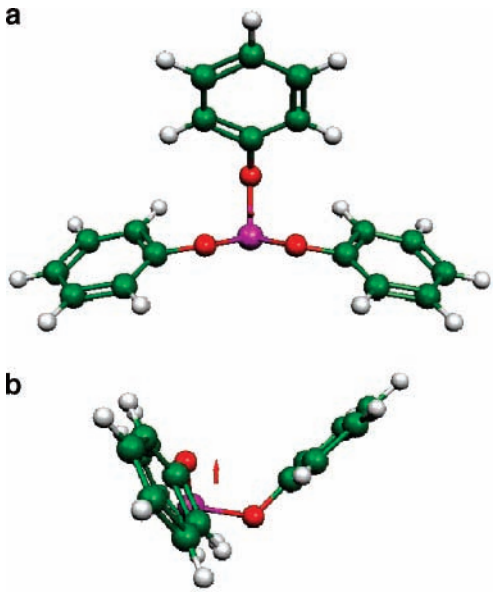

Figure 5. C_1 hexagonal TPP monomer after DFT calculations: (a) view along the dipole moment axis; (b) perpendicular view. The dipole moment is drawn.

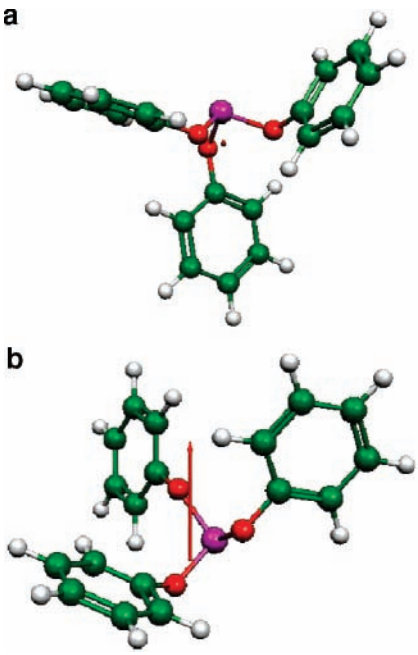

Figure 6. C_1 monoclinic TPP monomer after DFT calculations: (a) view along the dipole moment axis; (b) perpendicular view. The dipole moment is drawn.

significant (0.45 D) and directed along the *c*-axis, the direction of the molecular rods.

On the other hand, the optimized monoclinic C_1 structure (Figure 6) is more stable than the hexagonal one (difference in energy of 0.63 kcal/mol) and much more polar (1.44 D). The DFT optimizations of the monoclinic polymorph do not change significantly the dipolar properties, contrary to the hexagonal case. Interestingly, as underlined by Golovanov et al.,[30] the monoclinic C_1 form stems from the hexagonal C_1 one (or roughly from the C_s geometry) through variation of the τ and α angles (by 47.4° and 86.6°, respectively, in absolute values for one lateral phenoxy group) and is different from the most stable C_1 structure isolated in the gas state (that stems from the C_3 structure, see section 3.1) though very close in energy.

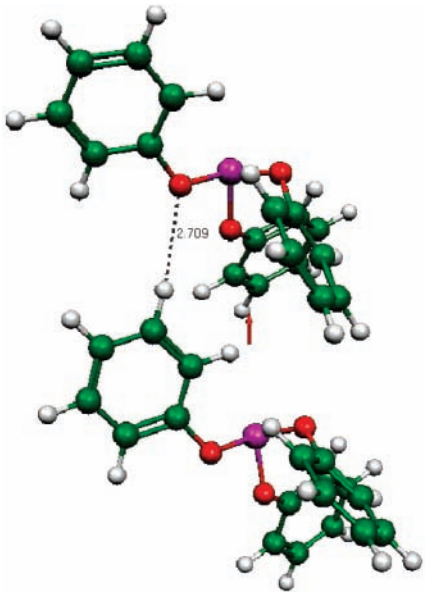

Figure 7. TPP dimer after DFT calculations. Short intermolecular C−H···O contacts are shown. The resulting dipole moment is drawn.

3.3. Weak Intermolecular C−H···O Hydrogen Bonding. In order to check the possibility of weak intermolecular C−H···O hydrogen bonds in TPP, that appear more and more—as explained in the Introduction—to be crucial, even though not taken into account at all by the other groups working on this topic,[7,12,14] we considered supramolecular moieties from the particular hexagonal crystal packing, which exhibits antiparallel infinite molecular rods directed along the *c*-axis and forming a hexagonal array. We carried out geometry optimizations on supermolecules initially constituted by assemblies of two and three TPP monomers directly selected from one molecular rod of the hexagonal crystal polymorph.[20] In this way the local environment of one probe molecule within these rods is simulated in terms of short/medium-range intermolecular interactions without using periodic DFT techniques, neglecting the influence of the surrounding parallel rods. The obtained optimized geometries are displayed in Figures 7 and 8.

After DFT optimizations at the MPW1PW91/6-311G** level, the packing remains roughly similar to the initial one, that is, the one occurring within one rod of the hexagonal crystal. However, one can underline that the P···P contact distances are longer (7.139 Å for the dimer, 6.963/6.578 Å for the trimer, versus 5.7286 Å— that is, the *c* cell parameter—within the hexagonal crystal) although a tendency for a closer packing seems to occur as the number *n* of constitutive molecules forming one rod increases. Correlatively, a helical dispersion of the stacking is observed as *n* increases when a rod is viewed along its axis. One can speculate that the strict molecular packing encountered within one rod of the hexagonal crystal is secured by the interactions with the surrounding parallel rods and not only by the intrarod intermolecular forces. As *n* increases, the resulting dipole moment diverges (0.28 D for the dimer, 1.01 D for the trimer) and remains parallel to the rod axis.

The shortest intrarod intermolecular contact in the dimeric species as well as in the trimeric species corresponds to a specific C−H···O contact, between an H atom in the meta position of a lateral (with respect to the molecular pseudomirror plane) phenoxy group and an O atom belonging to a lateral phenoxy group directly below (Figures 7 and 8). The associated contact distances (2.709 Å in the dimer; 2.594 and 2.646 Å in the trimer) are on the order of 2.7 Å, almost in the same range

TABLE 3: Geometric and Energetic Parameters of C−H···O Hydrogen Bonds in Simple Chemical Systems as Well as in TPP from MPW1PW91/6-311G Calculations**

system	C−H···O contact distance (Å)	C−H···O angle (deg)	ΔE interaction energy (kcal/mol)
benzene···OH_2	2.41	179.95	1.05
benzene···$(OH)_3P$	2.48	177.90	0.67
TPP···TPP (dimer)	2.709	168.157	1.2
TPP···TPP (trimer)	2.594, 2.646	161.235, 151.777	1.9

as the C−H···O intramolecular contacts (between 2.543 and 3.041 Å for the hexagonal C_1 geometry). These relatively short intermolecular C−H···O distances could be indicative of the occurrence of weak hydrogen bonding, the C−H···O angle being equal to 168.2° for the dimer and to 161.2° and 151.8° for the trimer. As is well-known, such an interaction is indeed favored when this angle is close to 180°.[31] Moreover, the computed interaction energy between the TPP monomers in the dimeric form is equal to 1.2 kcal/mol; it is on the order of magnitude of the energy of such a hydrogen bond. Indeed, we carried out calculations on simple models of C−H···O hydrogen-bonded systems, considering benzene and water as the interacting systems, as well as benzene and $P(OH)_3$. We found the following results reported in Table 3. The observed C−O···H distance in the TPP dimer is slightly longer than the computed one in the model systems, whereas the C−H···O angle is, as stressed above, not far from the ideal 180° value. The TPP···TPP interaction energy is higher than those of the model systems, especially that of the benzene···$(OH)_3P$ one. However, it is worth noting that the TPP···TPP interaction energy includes contributions other than the evidenced weak hydrogen bond, for example, other van der Waals interactions. For the TPP trimer we find also rather high interaction energy between the three TPP monomers, namely, 1.9 kcal/mol. All these results are in favor of the occurrence of weak C−H···O intermolecular hydrogen bonding for TPP within the molecular rods of the hexagonal crystal, as revealed by Raman spectroscopy and confirmed from the X-ray diffraction structural model.[22,20]

The intermolecular C−H···O H-bond evidenced in the present DFT study corresponds nicely to one of the two H-bonds previously reported in the hexagonal crystal,[20] namely, the H35···O3 contact of Figure 5 in ref 20 (2.9718 Å/109.04°). The other one (H15···O1, see Figure 5 in ref 20; 2.8136 Å/104.68°), also shown as relevant in the GS state transformed at 222 K,[23] involving two neighboring phenoxy groups perpendicular to the molecular pseudomirror plane, is not confirmed (3.432 Å/123.3° for the dimer).

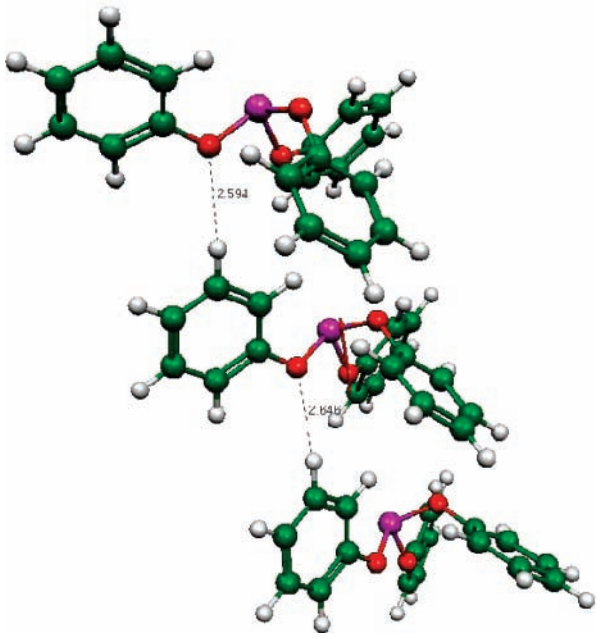

Figure 8. TPP trimer after DFT calculations. Short intermolecular C−H···O contacts are shown. The resulting dipole moment is drawn.

4. Conclusion

We have studied the TPP monomer in the gas state by the means of quantum chemistry DFT optimizations (mostly MPW1PW91/6-311G** calculations, Gaussian 03 software[28]). A new stable conformation (in this instance of C_1 symmetry) not yet encountered in the crystal states is revealed through the determination of the partial molecular potential energy surface. This geometry is characterized by a short H···O contact of 2.447 Å (C−H···O of 121.8°) that could be interpreted as an intramolecular hydrogen bond. It is shown that the conformational flexibility of TPP is huge, leading to the occurrence of different stable conformations very close in energy but displaying possibly different dipolar properties. The conformation of C_3 symmetry (symmetric propeller shape) turns out to be clearly the less stable. Furthermore, slight variations in the value of the torsion angles induce strong modifications of the amplitude and direction of the molecular dipole moment. The C_1 structure stems directly from the C_3 one through the variation of only two dihedral angles of the same phenoxy substituent. The C_1 form optimized from the monoclinic polymorph[30] (that stems directly from the C_s form also through the variation of only two dihedral angles of the same phenoxy substituent) is more stable (by 0.63 kcal/mol) and much more polar than the C_1 form optimized from the hexagonal polymorph[20] (similar to the ideal C_s geometry).

The molecular rod characteristic of the hexagonal crystal have been simulated with two and then three constitutive molecules (dimer and trimer, respectively), and the conformations of the supermolecular moieties have been optimized in the gas state (same type of DFT calculations as the above study of the monomer). A specific short C−H···O intermolecular contact displaying all the features of a weak hydrogen bond in terms of energy and geometric parameters has been isolated. This specific H-bond revealed in the present work nicely corresponds to one of the two C−H···O intrarod intermolecular H-bonds found in the hexagonal crystal.[20] Our study reveals qualitatively that weak C−H···O intermolecular H-bonds can definitely not be excluded in the hexagonal polymorph of TPP (and more generally in the other polymorphic modifications as well as in the GS) as interactions responsible for the supermolecular correlations, but we do not claim to give a precise geometric description of the H-bond network because our simulations have been performed with only three TPP molecules and at 0 K. The influence of the nearby parallel molecular rods as well as the temperature may indeed have a strong impact upon the characteristics of the hydrogen-bonding networks. It is shown that the trimer has a tendency for orientational ordering, but the strict molecular packing encountered within one rod of the hexagonal crystal requires apparently supplementary subtle interactions with the surrounding parallel rods.

When the biphasic nature of the GS is taken into account, it appears very difficult to analyze molecular conformations of TPP in the GS by experimental investigations. The use of microscopic (or nanoscopic) probes could allow us to discriminate the signals corresponding to the two different components of the GS. In this context, quantum chemistry calculations, or more generally numerical simulations, can be considered as an alternative tool to obtain information on the molecular conformation(s) encountered in the GS.

References and Notes

(1) Dunne, B. J.; Orpen, A. G. *Acta Crystallogr. C* **1991**, *47*, 345−347.

(2) Szlyk, E.; Szymanska, I. *Polyhedron* **1999**, *18*, 2941−2948.

(3) Ha, A.; Cohen, I.; Zhao, X.; Lee, M.; Kivelson, D. *J. Phys. Chem.* **1996**, *100*, 1−4.

(4) Cohen, I.; Ha, A.; Zhao, X.; Lee, M.; Fischer, T.; Strouse, M. J.; Kivelson, D. *J. Phys. Chem.* **1996**, *100*, 8518−8526.

(5) van Miltenburg, K.; Blok, K. *J. Phys. Chem.* **1996**, *100*, 16457−16459.

(6) Tarjus, G.; Alba-Simionesco, C.; Grousson, M.; Viot, P.; Kivelson, D. *J. Phys.: Condens. Matter* **2003**, *15*, S1077−S1084.

(7) Kivelson, D.; Tarjus, G. *J. Non-Cryst. Solids* **2002**, *307−310*, 630−636

(8) Alba-Simionesco, C.; Tarjus, G. *Europhys. Lett.* **2000**, *52*, 297−303.

(9) Tarjus, G.; Kivelson, S. A.; Nussinov, Z.; Viot, P. *J. Phys.: Condens. Matter* **2005**, *17*, R1143−R1182.

(10) Hédoux, A.; Guinet, Y.; Derollez, P.; Hernandez, O.; Paccou, L.; Descamps, M. *J. Non-Cryst. Solids* **2006**, *352*, 4994−5000.

(11) Hédoux, A.; Guinet, Y.; Derollez, P.; Hernandez, O.; Lefort, R.; Descamps, M. *Phys. Chem. Chem. Phys.* **2004**, *6*, 3192−3199.

(12) Tanaka, H.; Kurita, R.; Mataki, H. *Phys. Rev. Lett.* **2005**, *92*, 025701-1−025701-4.

(13) Tanaka, H. *Phys. Rev. E* **2000**, *62*, 6968−6976.

(14) Senker, J.; Sehnert, J.; Correll, S. *J. Am. Chem. Soc.* **2005**, *127*, 337−349.

(15) Senker, J.; Rössler, E. *Chem. Geol.* **2001**, *174*, 143−156.

(16) Dvinskikh, S.; Benini, G.; Senker, J.; Vogel, M.; Wiedersich, J.; Kudlik, A.; Rössler, E. *J. Phys. Chem. B* **1999**, *103*, 1727−1737.

(17) Wiedersich, J.; Kudlik, A.; Gottwald, J.; Benini, G.; Roggatz, I.; Rössler, E. *J. Phys. Chem. B* **1997**, *101*, 5800−5803.

(18) Johari, G. P.; Ferrari, C. *J. Phys. Chem. B* **1997**, *101*, 10191−10197.

(19) Senker, J.; Lüdecke, J. *Z. Naturforsch.* **2001**, *56b*, 1089−1099.

(20) Hernandez, O.; Hédoux, A.; Lefebvre, J.; Guinet, Y.; Descamps, M.; Papoular, R.; Masson, O. *J. Appl. Crystallogr.* **2002**, *35*, 212−219.

(21) Mizukami, M.; Kobashi, K.; Hanaya, M.; Oguni, M. *J. Phys. Chem. B* **1999**, *103*, 4078−4088.

(22) Guinet, Y.; Denicourt, T.; Hédoux, A.; Descamps, M. *J. Mol. Struct.* **2003**, *651−653*, 507−517.

(23) Derollez, P.; Hernandez, O.; Hédoux, A.; Guinet, Y; Masson, O.; Lefebvre, J.; Descamps, M. *J. Mol. Struct.* **2004**, *694*, 131−138.

(24) Mei, Q.; Ghalsasi, P.; Benmore, C. J.; Yarger, J. L. *J. Phys. Chem. B* **2004**, *108*, 20076−20082.

(25) Mei, Q.; Siewenie, J. E.; Benmore, C. J.; Ghalsasi, P.; Yarger, J. L. *J. Phys. Chem. B* **2006**, *110*, 9747−9750.

(26) Stephens, P. J.; Devlin, F. J.; Chabalowski, C. F.; Frisch, M. J. *J. Phys. Chem.* **1994**, *98*, 11623−11627.

(27) Adamo, C.; Barone, V. *J. Chem. Phys.* **1998**, *108*, 664−675.

(28) Frisch, M. J.; Trucks, G. W.; Schlegel, H. B.; Scuseria, G. E.; Robb, M. A.; Cheeseman, J. R.; Montgomery, J. A., Jr.; Vreven, T.; Kudin, K. N.; Burant, J. C.; Millam, J. M.; Iyengar, S. S.; Tomasi, J.; Barone, V.; Mennucci, B.; Cossi, M.; Scalmani, G.; Rega, N.; Petersson, G. A.; Nakatsuji, H.; Hada, M.; Ehara, M.; Toyota, K.; Fukuda, R.; Hasegawa, J.; Ishida, M.; Nakajima, T.; Honda, Y.; Kitao, O.; Nakai, H.; Klene, M.; Li, X.; Knox, J. E.; Hratchian, H. P.; Cross, J. B.; Bakken, V.; Adamo, C.; Jaramillo, J.; Gomperts, R.; Stratmann, R. E.; Yazyev, O.; Austin, A. J.; Cammi, R.; Pomelli, C.; Ochterski, J. W.; Ayala, P. Y.; Morokuma, K.; Voth, G. A.; Salvador, P.; Dannenberg, J. J.; Zakrzewski, V. G.; Dapprich, S.; Daniels, A. D.; Strain, M. C.; Farkas, O.; Malick, D. K.; Rabuck, A. D.; Raghavachari, K.; Foresman, J. B.; Ortiz, J. V.; Cui, Q.; Baboul, A. G.; Clifford, S.; Cioslowski, J.; Stefanov, B. B.; Liu, G.; Liashenko, A.; Piskorz, P.; Komaromi, I.; Martin, R. L.; Fox, D. J.; Keith, T.; Al-Laham, M. A.; Peng, C. Y.; Nanayakkara, A.; Challacombe, M.; Gill, P. M. W.; Johnson, B.; Chen, W.; Wong, M. W.; Gonzalez, C.; Pople, J. A. *Gaussian 03*, Revision B.04; Gaussian, Inc.: Pittsburgh, PA, 2003.

(29) Bondi, A. *J. Phys. Chem.* **1964**, *68*, 441−451.

(30) Golovanov, D. G.; Lyssenko, K. A.; Yu, Antipin, M.; Vygodskii, Y. S.; Lozinskaya, E. I.; Shaplov, A. S. *CrystEngComm* **2005**, *7*, 465−468.

(31) Desiraju, G. R. *Acc. Chem. Res.* **1996**, *29*, 441−449.